Electronic Supplementary Material (ESI) for CrystEngComm.
This journal is © The Royal Society of Chemistry 2015

Electronic Supplementary Information for:

Multiscale study of the cationic surfactants influence on amorphous calcium phosphate precipitation

A. Selmani[1], I. Coha[2], K. Magdić[2], B. Čolović[3], V. Jokanović[3], S. Šegota[2], S. Gajović[4], A. Gajović[5], D. Jurašin[6], M. Dutour Sikirić[6,*]

[1]Department of Chemistry, Faculty of Science, University of Zagreb, Horvatovac 102a, 10000 Zagreb, Croatia
[3]Vinča Institute of Nuclear Sciences, University of Belgrade, Mike Petrovića Alasa 11-14, 11 001 Belgrade, Serbia
[4]Croatian Institute for Brain Research, School of Medicine, University of Zagreb, Šalata 3, 10 000 Zagreb, Croatia
[2]Division for Marine and Environmental Research, [5]Division of Materials Physics and [6]Division of Physical Chemistry, Ruđer Bošković Institute, Bijenička cesta 54, 10 000 Zagreb, Croatia

*corresponding author:
Maja Dutour Sikirić
Laboratory for synthesis and self-assembly processes of organic molecules
Division of Physical Chemistry
Ruđer Bošković Institute
Bijenička cesta 54
10 000 ZagrebCroatia
e-mail: sikiric@irb.hr
Tel: + 385 1 456 0941

Content of listed material:

S1 Properties of surfactant/Na_2HPO_4 systems

S2 Surface tension measurements of surfactant/Na_2HPO_4 systems

S3 Size distribution by volume measured by dynamic light scattering (DLS) of DTAB and 12-2-12 micelles obtained in surfactant/Na_2HPO_4 systems.

S4 Raw data of the representative pH *vs.* time curves.

S5 Fourier transform infrared (FTIR) spectra of the precipitates formed in the control system after 10 min, 30 min and 24 h aging time.

S6 AFM images of large ACP particles and miceles

S7 DLS measurement of PNCs and polymeric asseblies of nanoclusters

S8 Size distribution of prenucleation clusters formed in the control precipitation system and in the presence of monomer and micellar concentrations of DTAB and 12-2-12 after 10 min aging time measured by atomic force microscopy (AFM).

S9 Size distribution of spherical ACP particles formed in the control precipitation system and in the presence of monomer and micellar concentrations of DTAB and 12-2-12 after 10 min aging time as measured from transmission electron microscope (TEM) micrographs.

S10 Size distribution by volume measured by dynamic light scattering (DLS) of chain-like aggregates of spherical ACP particles formed in the control precipitation system and in the presence of monomer and micellar concentrations of DTAB and 12-2-12 after 10 min aging time.

S11 Size distribution of prenucleation clusters formed in the control precipitation system and in the presence of monomer and micellar concentrations of DTAB and 12-2-12 after 30 min aging time measured by AFM.

S12 Size distribution of spherical ACP particles formed in the control precipitation system and in the presence of monomer and micellar concentrations of DTAB and 12-2-12 after 30 min aging time as measured from TEM micrographs.

S13 Size distribution by volume measured by DLS of chain-like aggregates of spherical ACP particles formed in the control precipitation system and in the presence of monomer and micellar concentrations of DTAB and 12-2-12 after 30 min aging time.

S14 FTIR spectra of precipitate formed in system containg spherical 12-2-12 micelles (DS2) after 30 min aging time.

S1 ***Properties of surfactant/Na_2HPO_4 systems.***

It is well established that the presence of an electrolyte in an aqueous solution of ionic surfactant can significantly alter its interfacial and micellization behavior due to screening of the ionic headgroups charge. As a result, the electrostatic repulsions between surfactants headgroups within the adsorbed monolayer and micelles are reduced.[1] Due to the reduction of electrostatic repulsions, critical micelle concentration of ionic surfactants in the presence of the electrolyte is usually lower. For the same reason, the size and the shape of the surfactant micelles can be affected by the presence of the electrolyte. The extent of the influence depends on the type and the concentration of electrolyte, as well as on the type of surfactant.[1] Therefore, the physicochemical properties of monomeric, DTAB, and dimeric, 12-2-12, surfactants in the presence of actual phosphate concentration in the CaP precipitation system were investigated.

Maximum surface excess concentrations, minimum areas per surfactant molecule and critical micelle concentrations obtained from surface tension measurements (Fig. S2†) are listed in Table 2. Γ_{max} (eqn 1) is a useful measure of the effectiveness of adsorption at the air/solution interface, since it is the maximum surfactant concentration that can be adsorbed. The effectiveness of adsorption is inversely proportional to a_{min} (eqn 2). Thus, the smaller the effective cross-sectional area of the surfactant headgroups at the air/solution interface, the greater the effectiveness of adsorption.[1] 12-2-12 molecule occupies larger area at air/solution interface than DTAB, as expected (Table 2). However, a_{min} values normalized to the number of dodecyl chains did not differ, meaning that monomer moiety in 12-2-12 molecule occupies the same area as DTAB molecule alone. As expected,[2,3] 12-2-12 was more efficient in lowering surface tension and had much lower cmc in comparison with DTAB (Table 2, Fig. S1a†). The difference in effectiveness of adsorption of DTAB and 12-2-12 was not as pronounced as was the difference in cmc.

The difference in surface behavior of these two surfactants was also illustrated by the shape of surface tension isotherms curves (Fig. S1†). In the case of DTAB, curve exhibits a typical course, that is, gradual decrease with an increase in surfactant concentration up to a plateau region, above which an almost constant γ value is obtained (Fig. 2a†). At concentration above cmc average hydrodynamic diameter and ζ potential of DTAB micelles were 3.6 ± 0.3 nm (Fig. S3a†) and 29.6 ± 2.5 mV, respectively. A number of studies have shown that, in the systems with no electrolyte added, DTAB forms small spherical micelles up to fairly high surfactant concentrations.[2,3] Even more, it was shown that the shape of the micelles does not change even at high electrolyte concentrations.[4] While the size of the DTAB

micelles was slightly larger in the presence of the Na_2HPO_4, their ζ potential, due to the phosphate counterion binding to the micelle/solution interface, was less positive compared to the micelles formed when no electrolyte was present.[3] From DLS measurements it is not possible to discern the shape of DTAB aggregates but having in mind literature data, [2,3,4] it is reasonable to assume the existence of spherical micelles in investigated DTAB system.

The shape of the 12-2-12 surface tension isotherm reveals a complex change in concentration and/or reorientation of molecules at the air/solution interface, which is paralled with the change of aggregate structure in the bulk (Fig. 2b†). The first break in γ *vs.* log c curve corresponds to the 12-2-12 cmc in the presence of Na_2HPO_4. Unlike DTAB, the surface tension of 12-2-12 continues to change with increasing concentration above cmc. The second break in the curve has been observed at the concentration corresponding to 12-2-12 cmc obtained without electrolyte.[2,3] DLS measurements showed that the value of hydrodynamic diameter of the 12-2-12 micelles increased with increasing surfactant concentration from 4.7 ± 0.5 nm immediately after the first break in surface tension isotherm (cmc) to 10.9 ± 0.4 nm at concentrations above 2nd break (Fig. S3b†). It has been shown that 12-2-12 at concentration close to cmc forms mainly spheroidal micelles, but a small increase in the surfactant concentration or addition of electrolyte results in the formation of elongated aggregates of lower curvature.[2] At concentrations above second break in surface tension curve, a bimodal distribution of 12-2-12 micelles ζ potential was observed (peaks at 14.2 ± 4.8 and 37.7 ± 7.3 mV). Two peaks in ζ potential distributions indicated the coexistence of differently charged and/or structured surfactant aggregates. In the case of dimeric cationic surfactant such a behavior is attributed to coexistence of spherical and cylindrical micelles.[5] Based on these observations it is reasonable to assume that at concentrations of 12-2-12 immediately above cmc spherical micelles were formed. With increasing surfactant concentration, at concentrations above 2nd break, spherical and elongated micelles coexisted.

References:

1. M. J. Rosen, *Surfactants and Interfacial Phenomena*, 3rd Ed, Wiley Interscience: Hoboken, New Jersey, 2004.

2. R. Zana, *Adv. Colloid Interface Sci.*, 2002, **97**, 205-253.

3. D. Jurašin, I. Habuš and N. Filipović-Vinceković, *Colloids Surf. A*, 2010, **368**, 119-128.

4. C.K. Liu and G. Warr, *Langmuir*, 2012, **28**, 11007-11016.

5. M. Pisárčik, M. Dubničková, F. Devínsky, I. Lacko and J. Škvarla, *Colloids Surf. A*, 1998,**143**, 69–75.

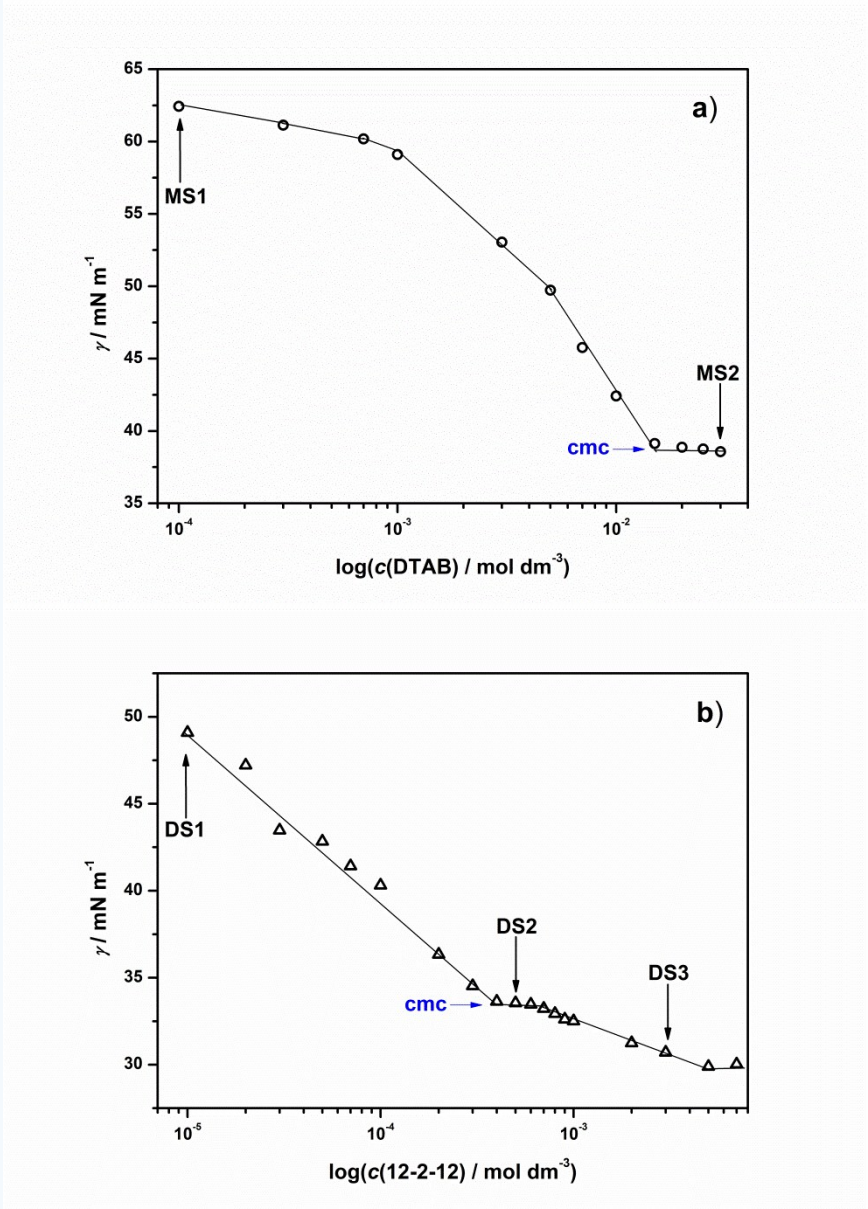

Fig. S2 Variation of surface tension (γ) with the concentration (c) for **a)** monomeric, DTAB and **b)** dimeric, 12-2-12 surfactant in the presence of $c(Na_2HPO_4) = 3 \cdot 10^{-3}$ mol dm^{-3}. pH_{init} = 7.4, θ / °C = (25 ±0.1). MS1, MS2, DS1, DS2 and DS3 denote surfactant concentration chosen for precipitation experiments (Table 1), cmc denotes critical micelle concentration of surfactants. The lines are only guidance for an eye.

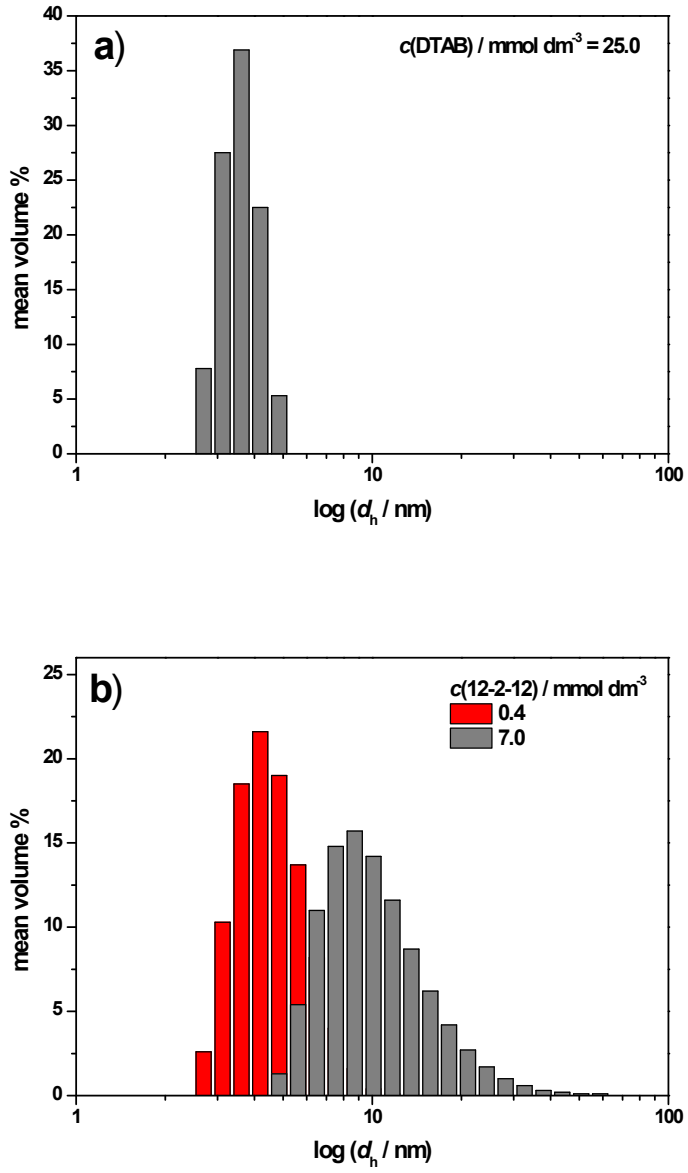

Fig. S3 Size distribution by volume measured by dynamic light scattering (DLS) of **a)** DTAB and **b)** 12-2-12 micelles obtained in the presence of electrolyte, $c(Na_2HPO_4)$ = 3 · 10^{-3} mol dm^{-3}. pH_{init} = 7.4, θ / °C = (25 ±0.1). Actual surfactant concentrations are denoted.

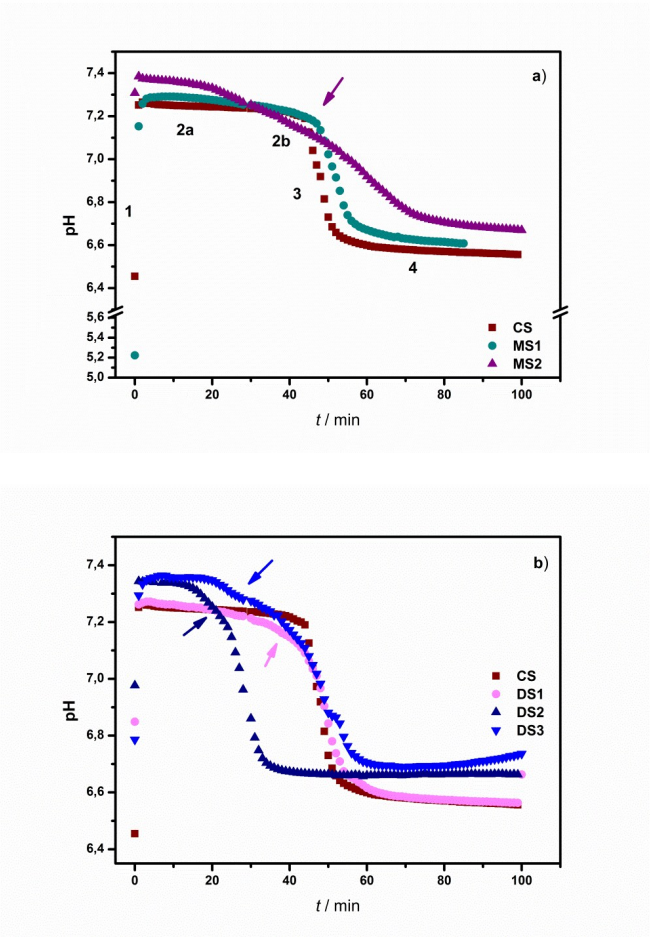

Fig. S4 Raw data of the representative pH *vs.* time curve of amorphous calcium phosphate (ACP) formation and transformation in the absence (CS) and presence of monomer and micellar concentrations of a) DTAB (MS1 and MS2) and b) 12-2-12 (DS1, DS2 and DS3).

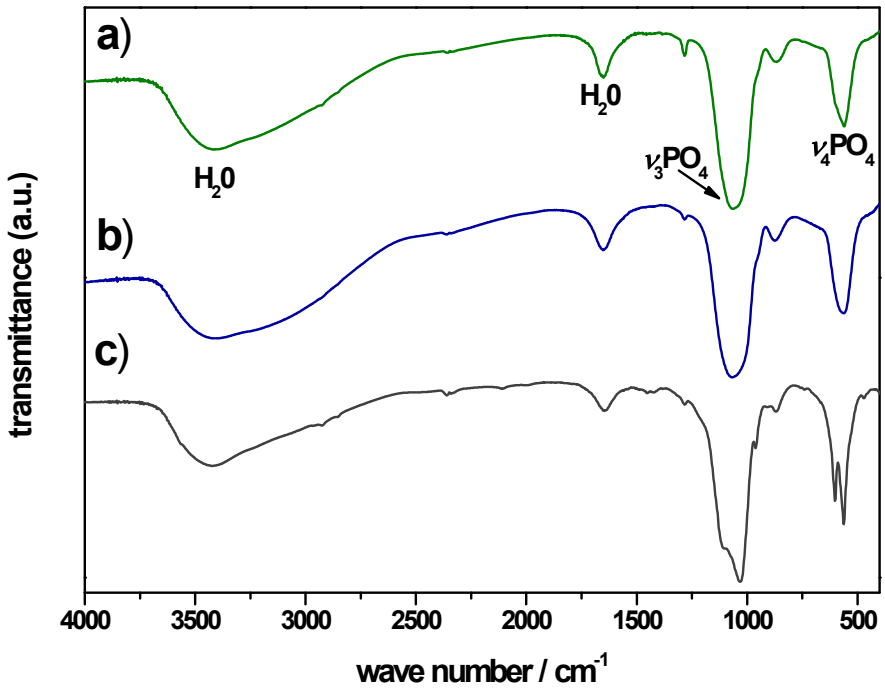

Fig. S5 Fourier transform infrared (FTIR) spectra of the precipitates formed in the control system ($c(CaCl_2) = c(Na_2HPO_4) = 3 \cdot 10^{-3}$ mol dm^{-3}, $pH_{init} = 7.4$, θ / °C = (25 ±0.1). after **a)** 10 min, **b)** 30 min and **c)** 24 h aging time.

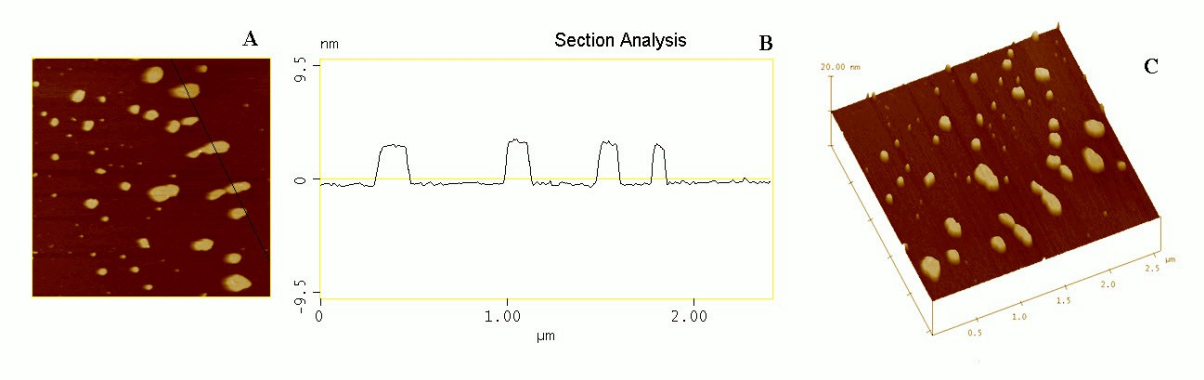

Fig. S6 Atomic force microscopy topographic view (A), section profile (B) and 3D view of the particles formed in the presence of DTAB monomers (MS1) after 10 minutes aging time. pH_{init} = 7.4, θ / °C = (25 ±0.1). The sample is presented on 2.5 µm × 2.5 µm surface area with vertical scale 20 nm

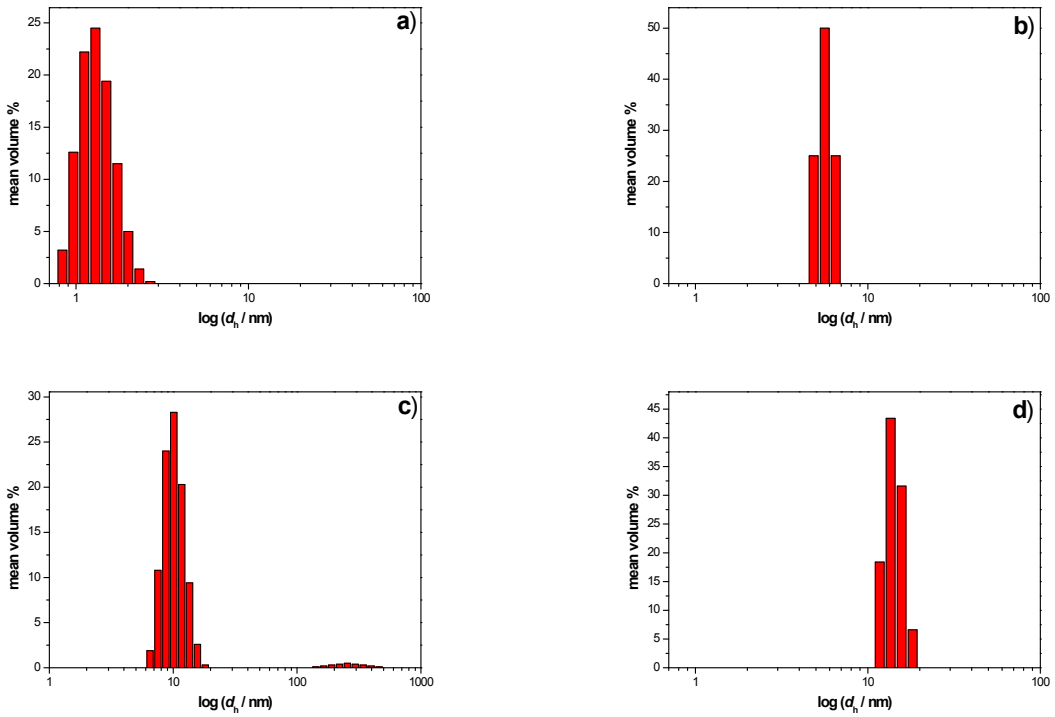

Fig. S7 In order to confirm AFM results, control sample after 30 min aging time was centrifugated at 6000 rps (Hettich EBA 8) for 5 min. Size distribution of particles was measured in 70 successive runs each lasting 10 s. Results were not averaged. Representative runs for the particles of the sizes less than 20 nms are shown.

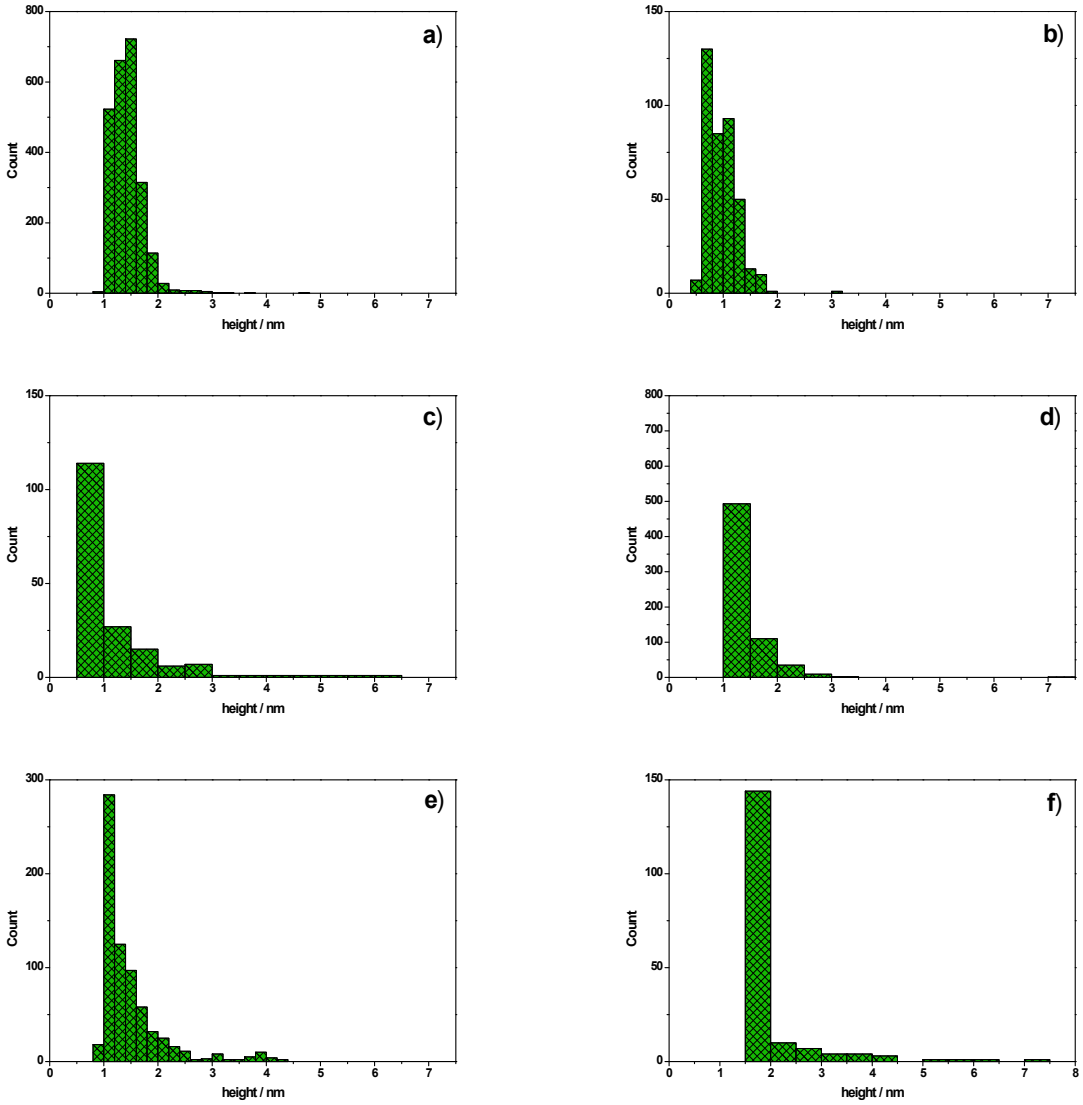

Fig. S8 Size distribution of prenucleation clusters, measured by atomic force microscopy (AFM), formed after 10 min aging time in **a) CS: control system** $c(CaCl_2) = c(Na_2HPO_4) = 3 \cdot 10^{-3}$ mol dm^{-3}; **b) MS1:** c(DTAB) = $1 \cdot 10^{-4}$ mol dm^{-3}; **c) MS2:** c(DTAB) = $3 \cdot 10^{-2}$ mol dm^{-3}; **d) DS1:** c(12-2-12) = $1 \cdot 10^{-5}$ mol dm^{-3}; **e) DS2:** c(12-2-12) = $5 \cdot 10^{-4}$ mol dm^{-3}; **f) DS3:** c(12-2-12) = $3 \cdot 10^{-3}$ mol dm^{-3}. pH_{init} = 7.4, θ / °C = (25 ±0.1).

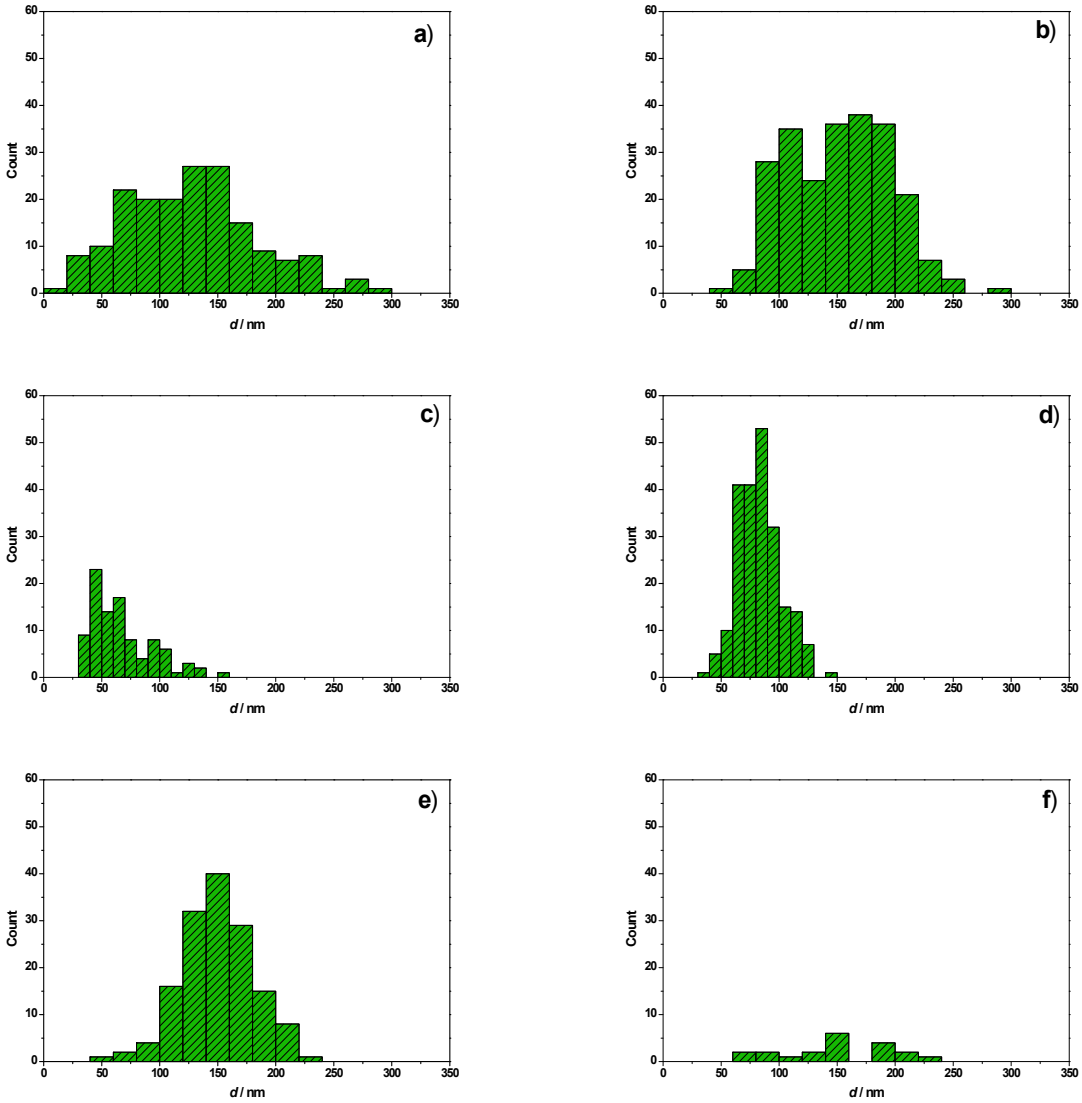

Fig. S9 Size distribution of spherical ACP particles as measured from transmission electron microscope (TEM) micrographs formed after 10 min aging time in **a) CS: control system** $c(CaCl_2) = c(Na_2HPO_4) = 3 \cdot 10^{-3}$ mol dm^{-3}; **b) MS1:** c(DTAB) = $1 \cdot 10^{-4}$ mol dm^{-3}; **c) MS2:** c(DTAB) = $3 \cdot 10^{-2}$ mol dm^{-3}; **d) DS1:** c(12-2-12) = $1 \cdot 10^{-5}$ mol dm^{-3}; **e) DS2:** c(12-2-12) = $5 \cdot 10^{-4}$ mol dm^{-3}; **f) DS3:** c(12-2-12) = $3 \cdot 10^{-3}$ mol dm^{-3}. pH_{init} = 7.4, θ / °C = (25 ±0.1).

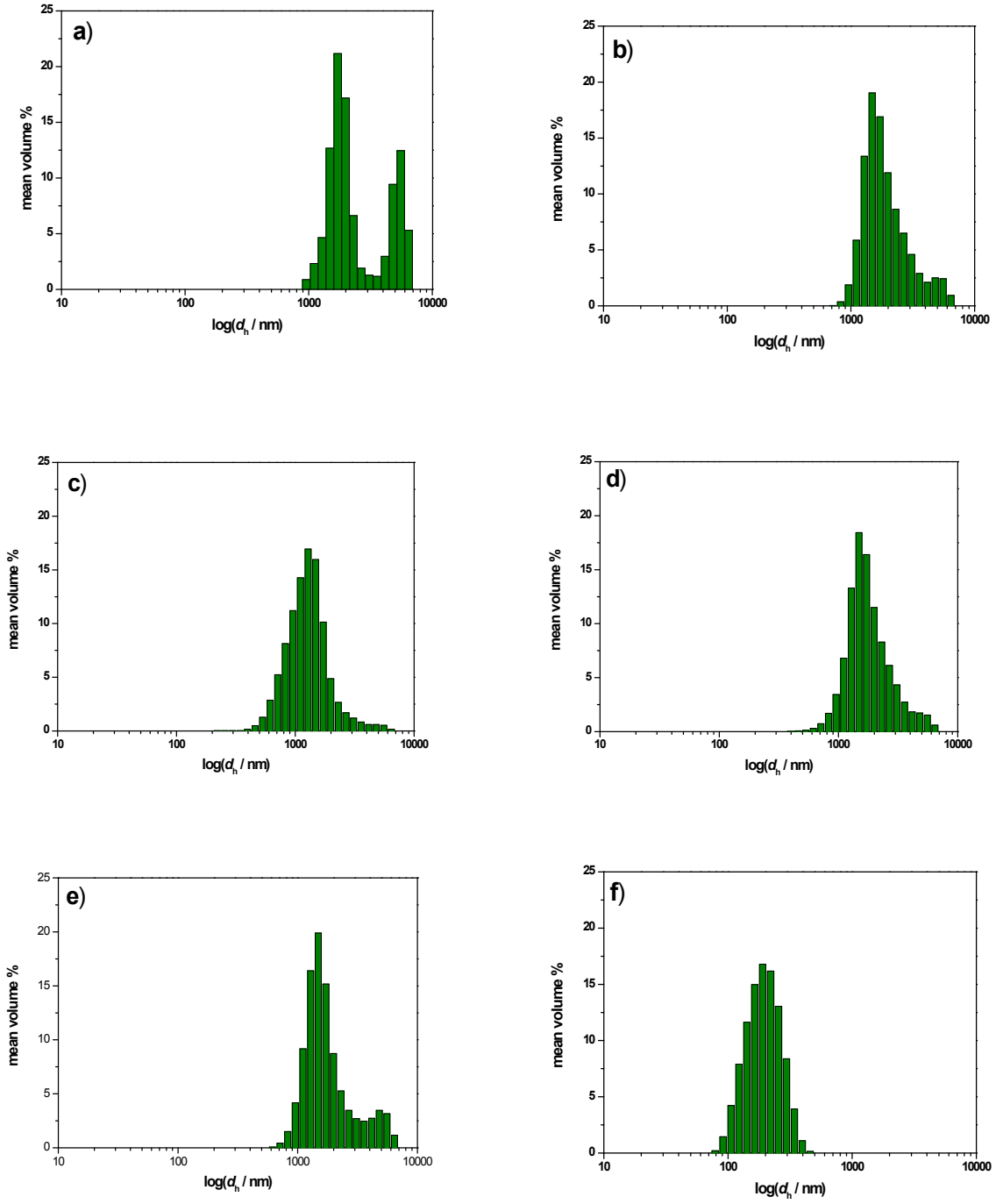

Fig. S10 Size distribution by volume of chain-like aggregates of spherical ACP particles, measured by dynamic light scattering (DLS), formed after 10 min aging time in **a) CS: control system** $c(CaCl_2) = c(Na_2HPO_4) = 3 \cdot 10^{-3}$ mol dm^{-3}; **b) MS1:** c(DTAB) = $1 \cdot 10^{-4}$ mol dm^{-3}; **c) MS2:** c(DTAB) = $3 \cdot 10^{-2}$ mol dm^{-3}; **d) DS1:** c(12-2-12) = $1 \cdot 10^{-5}$ mol dm^{-3}; **e) DS2:** c(12-2-12) = $5 \cdot 10^{-4}$ mol dm^{-3}; **f) DS3:** c(12-2-12) = $3 \cdot 10^{-3}$ mol dm^{-3}. pH_{init} = 7.4, θ / °C = (25 ±0.1).

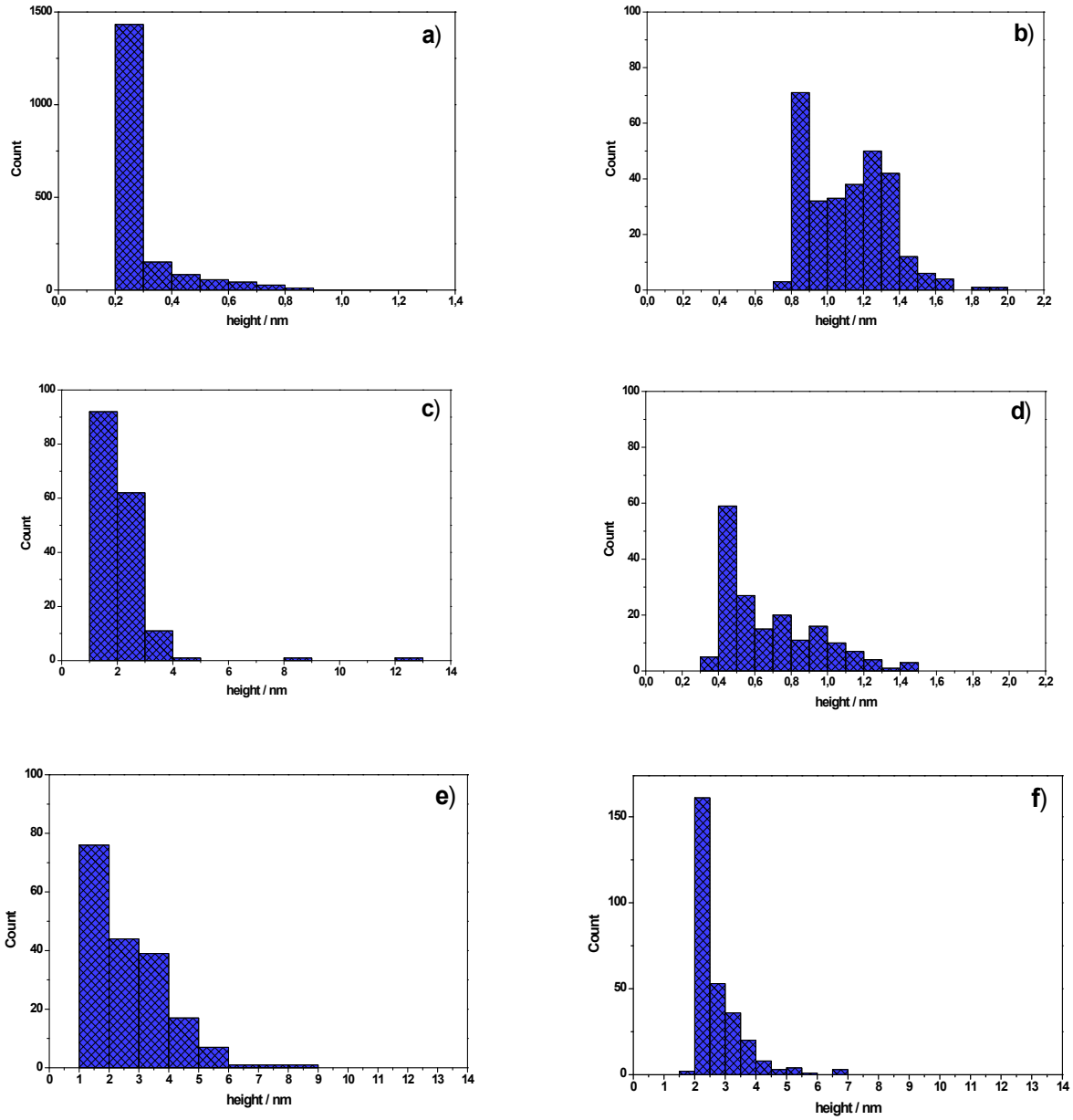

Fig. S11 Size distribution of prenucleation clusters, measured by atomic force microscopy (AFM), formed after 30 min aging time in **a) CS: control system** $c(CaCl_2) = c(Na_2HPO_4) = 3 \cdot 10^{-3}$ mol dm^{-3}; **b) MS1:** c(DTAB) = $1 \cdot 10^{-4}$ mol dm^{-3}; **c) MS2:** c(DTAB) = $3 \cdot 10^{-2}$ mol dm^{-3}; **d) DS1:** c(12-2-12) = $1 \cdot 10^{-5}$ mol dm^{-3}; **e) DS2:** c(12-2-12) = $5 \cdot 10^{-4}$ mol dm^{-3}; **f) DS3:** c(12-2-12) = $3 \cdot 10^{-3}$ mol dm^{-3}. pH_{init} = 7.4, θ / °C = (25 ±0.1).

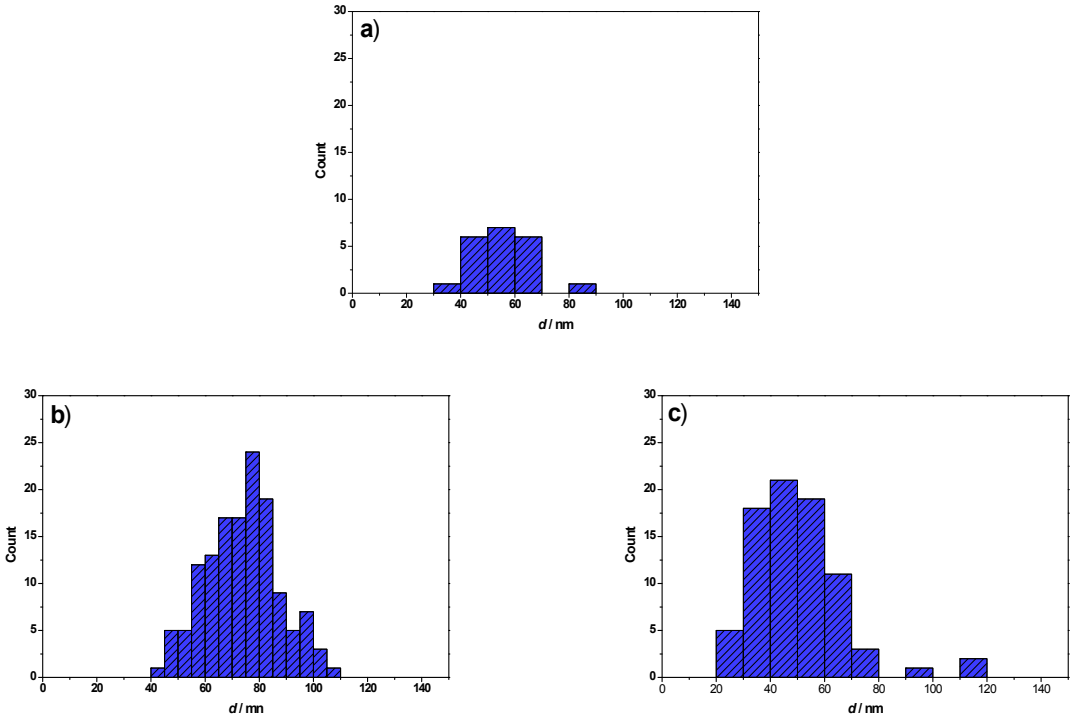

Fig. S12 Size distribution of spherical ACP particles formed after 30 min aging time as measured from transmission electron microscope (TEM) micrographs in **a) CS: control system** $c(CaCl_2) = c(Na_2HPO_4) = 3 \cdot 10^{-3}$ mol dm^{-3}; **b) MS1:** c(DTAB) = $1 \cdot 10^{-4}$ mol dm^{-3}; **c) MS2:** c(DTAB) = $3 \cdot 10^{-2}$ mol dm^{-3}; **d) DS1:** c(12-2-12) = $1 \cdot 10^{-5}$ mol dm^{-3}; **e) DS2:** c(12-2-12) = $5 \cdot 10^{-4}$ mol dm^{-3}; **f) DS3**: c(12-2-12) = $3 \cdot 10^{-3}$ mol dm^{-3}. pH_{init} = 7.4, θ / °C = (25 ±0.1).

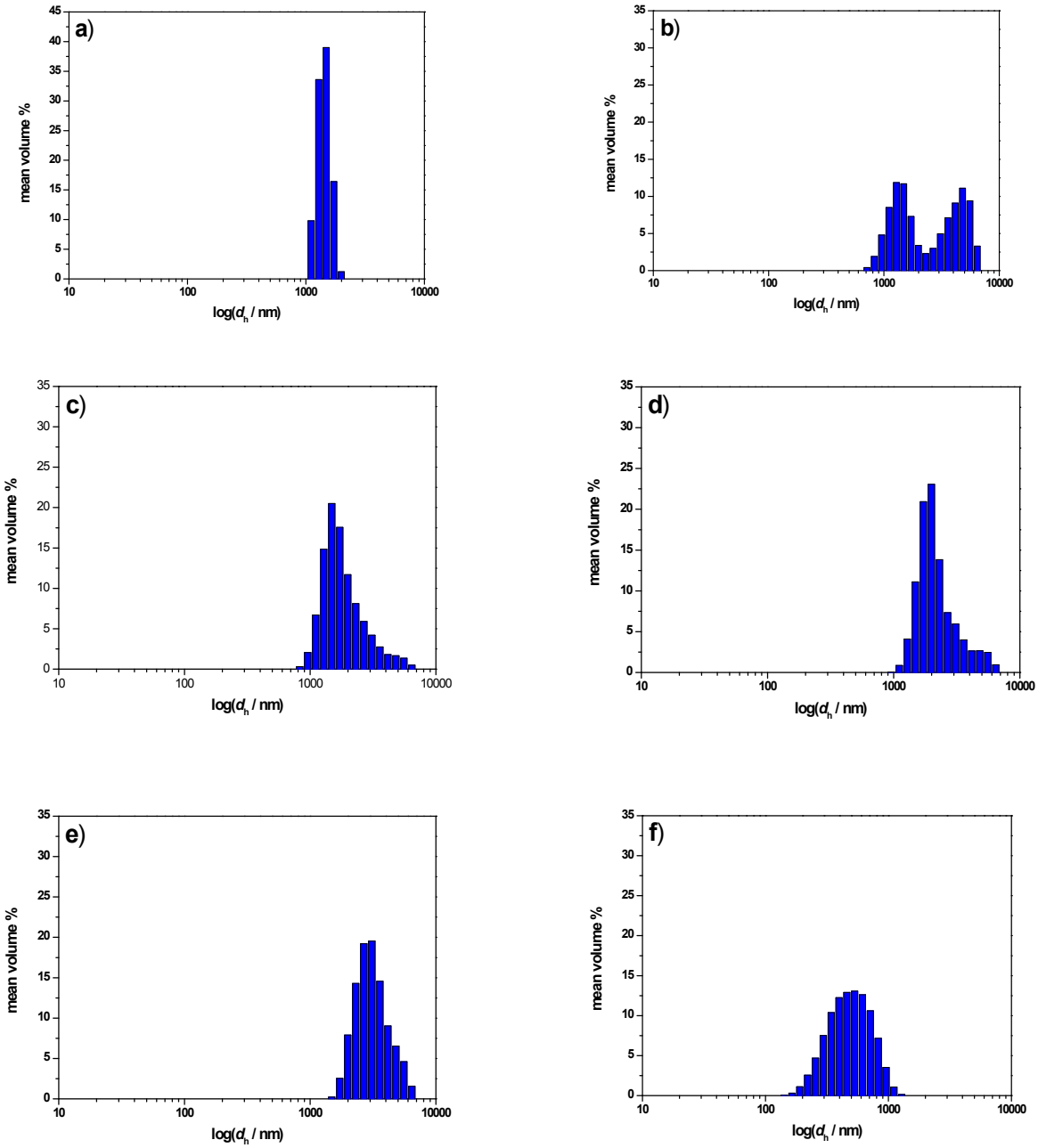

Fig. S13 Size distribution by volume of chain-like aggregates of spherical ACP particles, measured by dynamic light scattering (DLS), formed after 30 min aging time **a) CS: control system** $c(CaCl_2) = c(Na_2HPO_4) = 3 \cdot 10^{-3}$ mol dm^{-3}; **b) MS1:** c(DTAB) = $1 \cdot 10^{-4}$ mol dm^{-3}; **c) MS2:** c(DTAB) = $3 \cdot 10^{-2}$ mol dm^{-3}; **d) DS1:** c(12-2-12) = $1 \cdot 10^{-5}$ mol dm^{-3}; **e) DS2:** c(12-2-12) = $5 \cdot 10^{-4}$ mol dm^{-3}; **f) DS3:** c(12-2-12) = $3 \cdot 10^{-3}$ mol dm^{-3}. pH_{init} = 7.4, θ / °C = (25 ±0.1).

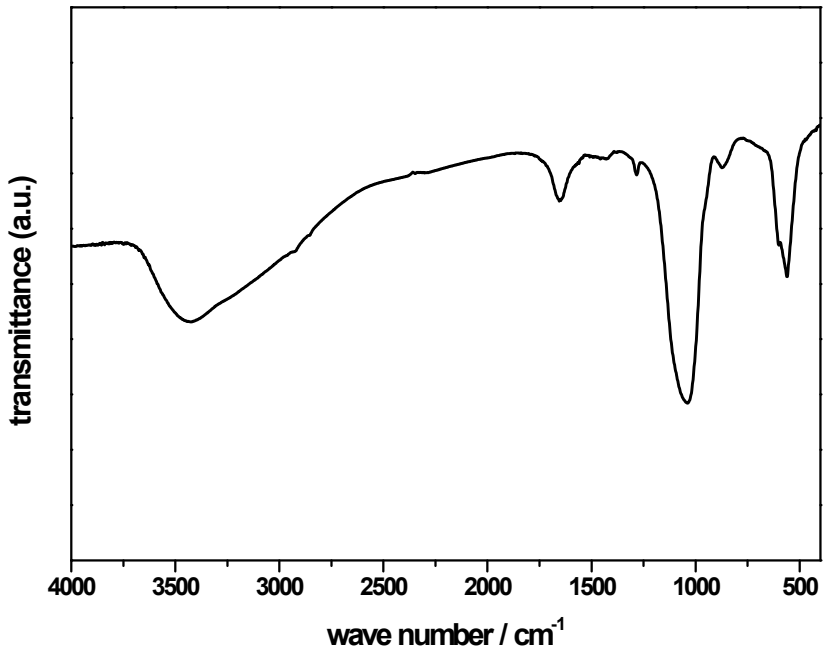

Fig. S14 Fourier transform infrared spectra (FTIR) of the precipitate formed after 30 min aging time in the system containing sperical 12-2-12 micelles (DS2), $c(CaCl_2) = c(Na_2HPO_4) = 3 \cdot 10^{-3}$ mol dm^{-3}, c(12-2-12) = $5 \cdot 10^{-4}$ mol dm^{-3}, pH_{init} = 7.4, θ / °C = (25 ±0.1).